Journal of Crystal Growth 483 (2018) 200–205

Contents lists available at ScienceDirect

Journal of Crystal Growth

journal homepage: www.elsevier.com/locate/crys

Study on growth techniques and macro defects of large-size Nd:YAG laser crystal

Jiliang Quan [a,c], Xin Yang [a], Mingming Yang [a], Decai Ma [b], Jinqiang Huang [c], Yunzhong Zhu [b,*], Biao Wang [a,b,*]

[a] State Key Laboratory of Optoelectronic Materials and Technologies/Institute of Optoelectronic and Functional Composite Materials, School of Physics and Engineering, Sun Yat-sen University, Guangzhou 510275, China
[b] Sino French Institute of Nuclear Engineering and Technology, Sun Yat-sen University, Zhuhai 519082, China
[c] Guangzhou Semiconductor Material Academy, Guangzhou 510610, China

ARTICLE INFO

Article history:
Received 29 June 2017
Received in revised form 30 November 2017
Accepted 3 December 2017
Available online 5 December 2017
Communicated by K. Jacobs

Keywords:
A2. Single crystal growth
A2. Czochralski method
A2. Large size
A1. Defects
B1. Nd:YAG
B1. Oxides

ABSTRACT

Large-size neodymium-doped yttrium aluminum garnet (Nd:YAG) single crystals were grown by the Czochralski method. The extinction ratio and wavefront distortion of the crystal were tested to determine the optical homogeneity. Moreover, under different growth conditions, the macro defects of inclusion, striations, and cracking in the as-grown Nd:YAG crystals were analyzed. Specifically, the inclusion defects were characterized using scanning electron microscopy and energy dispersive spectroscopy. The stresses of growth striations and cracking were studied via a parallel plane polariscope. These results demonstrate that improper growth parameters and temperature fields can enhance defects significantly. Thus, by adjusting the growth parameters and optimizing the thermal environment, high-optical-quality Nd:YAG crystals with a diameter of 80 mm and a total length of 400 mm have been obtained successfully.
© 2017 Elsevier B.V. All rights reserved.

1. Introduction

Because of the important role of lasers in industrial, medical, and scientific fields, the high power solid-state laser has attracted great attention [1–5]. In the past decade, the average power output of solid-state lasers has increased from 1 to 10 kW; it is even expected to reach 100 kW. However, as the core material in solid-state laser devices, the performance of laser crystals cannot meet the development needs of solid-state laser technology. Specifically, the study of large-size crystals for high power lasers has developed slowly; additionally, the optical quality of laser crystals is poor. Neodymium-doped yttrium aluminum garnet (Nd:YAG) crystals are the most commonly used active medium in high-power continuous and average power pulse solid-state lasers [6–8]. Because of its excellent properties, including optical uniformity, high gain, and the small radial concentration gradient of the Nd^{3+} ion, Nd:YAG has become the pillar material for producing high-power solid state lasers. Large-diameter Nd:YAG crystals not only meet the quality requirements of large-size laser rods and slabs, but also improve the production efficiency of a single crystal boule.

It is difficult to achieve mass production of large-size, high-quality Nd:YAG crystals due to the inaccessibility of certain growth conditions, such as high growth temperature, serious component segregation of the Nd^{3+} ion, solid solution limit, easy crack formation, and the presence of the core and lateral. Although studies on the growth of Nd:YAG crystals have been carried out for more than 40 years, there have been few reports focusing on the growth of large-diameter Nd:YAG crystals, and more attention has been bestowed upon its laser properties. Only a few studies focusing on ϕ 50 mm Nd:YAG [9], the high Nd^{3+} concentration [10], crystal defects [7,11–18], and growth simulation [19] of Nd:YAG crystals have been reported. The actual temperature field is too complicated for computer simulation; therefore, limited quantitative studies on the growth of large-size Nd:YAG crystals have been reported. Furthermore, important issues, such as suitable temperature field and optimum growth parameters, remain unsolved. The correlation studies on the growth and properties of large-size Nd:YAG laser crystals offer significant academic and economic benefit. In this paper, to solve the above issues, we studied the temperature field and growth mechanism of large-size Nd:YAG crystals. The

* Corresponding authors at: State Key Laboratory of Optoelectronic Materials and Technologies/Institute of Optoelectronic and Functional Composite Materials, School of Physics and Engineering, Sun Yat-sen University, Guangzhou 510275, China; Sino French Institute of Nuclear Engineering and Technology, Sun Yat-sen University, Zhuhai 519082, China.
E-mail addresses: zhuyzh7@mail.sysu.edu.cn (Y. Zhu), wangbiao@mail.sysu.edu.cn (B. Wang).

https://doi.org/10.1016/j.jcrysgro.2017.12.004
0022-0248/© 2017 Elsevier B.V. All rights reserved.

issues of inclusions, cracks, and other defects in the growth of crystals were addressed. Thus, Nd:YAG laser crystals of 80 mm diameter were successfully grown.

2. Materials and methods

Nd:YAG laser crystals with a doping concentration of 1 at% Nd^{+3} were grown by the conventional Czochralski (CZ) method using a radio frequency (RF) induction heater. The raw powders of Y_2O_3 (5N), Al_2O_3 (5N), and Nd_2O_3 (6N) were adequately mixed in the stoichiometric ratio, then pressed into a cylinder and calcined at 1300 °C for 24 h. An iridium crucible (180 mm diameter, 200 mm height) was chosen as the heating element. The crucible was surrounded by an isolated zirconia cylinder. Then, the multilayer zirconium oxide and ceramic materials were aligned in a double wall structure. The suitable relative height between the induction coil and the crucible was modulated to achieve a high temperature gradient and the optimal thermal field to grow large-size Nd:YAG crystals. The entire growth process was performed in argon shielding gas. During crystal growth, high precision in temperature was realized using a 2404 type Eurotherm temperature control system. The temperatures above melt (0, 5, 10 mm from the melt surface) were measured by Ir-Rh thermocouples. A computer simulation was also performed.

Next, an oriented Nd:YAG crystal was employed as the seed crystal. The raw materials in the crucible were then melted at ~1970 °C. After placing the seeds into the melt, changes in the crystallization front were monitored carefully. The suitable seeding temperature was determined after seeding down several times. This seeding temperature corresponds to the temperature at which the weight of the seed remains constant and the seed undergoes microfusion. The crystal growth program was then turned into the automatic diameter controlled (ADC) function to start body control. During the growth process, a pulling rate of 0.5–0.8 mm/h and a rotation rate of 12–18 rpm were employed.

The stress (induced by the defects) that affects the crystal quality was studied by a parallel plane polariscope (PSV-201). The extinction ratio and wavefront distortion of the as-grown crystals were studied with an extinction ratio meter (ER2000) and laser interferometer (G30D). Inclusion defects, in the transversely sliced and polished crystal cylinder, could be revealed by scanning electron microscopy (SEM). The chemical compositions of the defective area were characterized by an energy dispersive spectrometer (EDS).

3. Results and discussion

A series of defects, such as cracks, color center, inclusions, etc. often emerges during the growth of a large-diameter Nd:YAG crystal, which significantly degrades the crystal quality and limits productivity. To understand the mechanism behind the generation of these macro defects, we grew numerous Nd:YAG crystals under different growth conditions. Figs. 1–3 present the defective ones grown in the early stage of our study.

Fig. 1a shows a crystal interface that suddenly melted-off. The tail portion indicates that the crystal/melt interface tends to form a concave shape toward the melt. It is important to note that, during the growth of the as-grown crystal, the ADC system does not present any abnormal sudden weight or temperature changes. Also in Fig. 1a, obvious growth striations are observed in the region from the shoulder to the cylindrical part of the crystal. The striations and diameter variations correspond with the observed growth rate fluctuations during the growth process [20]. Moreover, as shown in Fig. 1b and c, the crystal exhibits a wide central core with high tension. These results indicate that the inducement of

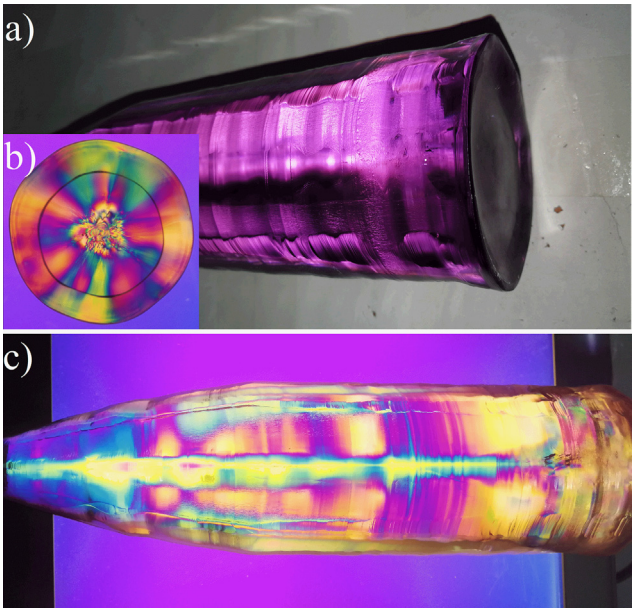

Fig. 1. (a) Nd:YAG boule which processes growth striations and the concave growth interface. (b) Longitudinal parallel-plane polariscopic image of the end face of the crystal. (c) Transverse parallel-plane polariscopic image of the crystal.

defects can be attributed to the inappropriate temperature field of the solid-liquid interface.

In the CZ method, crystal growth is initiated at the solid-liquid interface; the latent heat of crystallization is released through the solid-liquid interface as well. A variety of defects is produced when the crystal is grown in an unsuitable temperature field. Furthermore, the temperature and convection distribution determine the shape of the solid-liquid interface. Thus, a proper melt/crystal interface is important to obtain high-quality single crystals. To change the temperature distribution, we adjusted the relative vertical height between the iridium crucible and the RF coil, and decreased the insulation effect (of the thermal insulation) above the crucible to increase the temperature gradient along the growth direction. In addition to the intuitive approach of changing the thermal insulation, the crystal rotation rate also determines the convection and temperature fields of CZ melt [21]. As the crystal rotation rate increases and the vertical temperature gradient decreases, the interface shape can change from convex to concave toward the melt [21–23]. Approaching the problem from this point of view, in order to reduce the forced convection, we changed the rotation rate from 16 to 14 rpm gradually in the cylindrical part. Finally, we modulated the temperature gradient above the melt from −1 °C/mm to 25 °C/mm; the temperature gradient of the solid-liquid interface was then effectively improved.

Fig. 2a shows the different-sized and irregularly shaped inclusions inside the crystal. The polariscopic image (Fig. 2b) of the crystal exhibits a wide area comprised of a central core, inclusions, and precipitated compositions, which implies poor optical quality. In order to thoroughly examine these defects, the crystal boule was cut and polished along the ⟨1 1 1⟩ direction. Fig. 2c and d present SEM images of the polished ⟨1 1 1⟩ slice. In these figures, cloud and flake-like inclusions are observed. In Fig. 2c, positions 1 and 2 were examined using EDS to compare the composition differences between the inclusions and normal crystallization region. Table 1 illustrates the results of the EDS measurements. The primary elements of C, O, Al, and Y, and the impurity elements of Ta and Ir were found in parcel zone 1. Obviously, position 1 contains more evaporated carbon than position 2, which indicates that position 1 contains cavities. The impurities, Ta and Ir, originate

Download English Version:

https://daneshyari.com/en/article/8148952

Download Persian Version:

https://daneshyari.com/article/8148952

Daneshyari.com